

Studying Parton Energy Loss in Heavy-Ion Collisions via Direct-Photon and Charged-Particle Azimuthal Correlations

B. I. Abelev,⁸ M. M. Aggarwal,³⁰ Z. Ahammed,⁴⁷ A. V. Alakhverdyants,¹⁷ B. D. Anderson,¹⁸ D. Arkhipkin,³ G. S. Averichev,¹⁷ J. Balewski,²² L. S. Barnby,² S. Baumgart,⁵² D. R. Beavis,³ R. Bellwied,⁵⁰ F. Benedosso,²⁷ M. J. Betancourt,²² R. R. Betts,⁸ A. Bhasin,¹⁶ A. K. Bhati,³⁰ H. Bichsel,⁴⁹ J. Bielcik,¹⁰ J. Bielcikova,¹¹ B. Biritz,⁶ L. C. Bland,³ B. E. Bonner,³⁶ J. Bouchet,¹⁸ E. Braidot,²⁷ A. V. Brandin,²⁵ A. Bridgeman,¹ E. Bruna,⁵² S. Bueltmann,²⁹ I. Bunzarov,¹⁷ T. P. Burton,² X. Z. Cai,⁴⁰ H. Caines,⁵² M. Calderón de la Barca Sánchez,⁵ O. Catu,⁵² D. Cebra,⁵ R. Cendejas,⁶ M. C. Cervantes,⁴² Z. Chajecki,²⁸ P. Chaloupka,¹¹ S. Chattopadhyay,⁴⁷ H. F. Chen,³⁸ J. H. Chen,⁴⁰ J. Y. Chen,⁵¹ J. Cheng,⁴⁴ M. Cherney,⁹ A. Chikanian,⁵² K. E. Choi,³⁴ W. Christie,³ P. Chung,¹¹ R. F. Clarke,⁴² M. J. M. Codrington,⁴² R. Corliss,²² J. G. Cramer,⁴⁹ H. J. Crawford,⁴ D. Das,⁵ S. Dash,¹³ A. Davila Leyva,⁴³ L. C. De Silva,⁵⁰ R. R. Debbé,³ T. G. Dedovich,¹⁷ M. DePhillips,³ A. A. Derevschikov,³² R. Derradi de Souza,⁷ L. Didenko,³ P. Djawotho,⁴² S. M. Dogra,¹⁶ X. Dong,²¹ J. L. Drachenberg,⁴² J. E. Draper,⁵ J. C. Dunlop,³ M. R. Dutta Mazumdar,⁴⁷ L. G. Efimov,¹⁷ E. Elhalhuli,² M. Elnimr,⁵⁰ J. Engelage,⁴ G. Eppley,³⁶ B. Erazmus,⁴¹ M. Estienne,⁴¹ L. Eun,³¹ O. Evdokimov,⁸ P. Fachini,³ R. Fatemi,¹⁹ J. Fedorisin,¹⁷ R. G. Fersch,¹⁹ P. Filip,¹⁷ E. Finch,⁵² V. Fine,³ Y. Fisyak,³ C. A. Gagliardi,⁴² D. R. Gangadharan,⁶ M. S. Ganti,⁴⁷ E. J. Garcia-Solis,⁸ A. Geromitsos,⁴¹ F. Geurts,³⁶ V. Ghazikhanian,⁶ P. Ghosh,⁴⁷ Y. N. Gorbunov,⁹ A. Gordon,³ O. Grebenyuk,²¹ D. Grosnick,⁴⁶ B. Grube,³⁴ S. M. Guertin,⁶ A. Gupta,¹⁶ N. Gupta,¹⁶ W. Guryn,³ B. Haag,⁵ T. J. Hallman,³ A. Hamed,⁴² L.-X. Han,⁴⁰ J. W. Harris,⁵² J. P. Hays-Wehle,²² M. Heinz,⁵² S. Heppelmann,³¹ A. Hirsch,³³ E. Hjort,²¹ A. M. Hoffman,²² G. W. Hoffmann,⁴³ D. J. Hofman,⁸ R. S. Hollis,⁸ H. Z. Huang,⁶ T. J. Humanic,²⁸ L. Huo,⁴² G. Igo,⁶ A. Iordanova,⁸ P. Jacobs,²¹ W. W. Jacobs,¹⁵ P. Jakl,¹¹ C. Jena,¹³ F. Jin,⁴⁰ C. L. Jones,²² P. G. Jones,² J. Joseph,¹⁸ E. G. Judd,⁴ S. Kabana,⁴¹ K. Kajimoto,⁴³ K. Kang,⁴⁴ J. Kapitan,¹¹ K. Kauder,⁸ D. Keane,¹⁸ A. Kechechyan,¹⁷ D. Kettler,⁴⁹ D. P. Kikola,²¹ J. Kiryluk,²¹ A. Kisiel,⁴⁸ S. R. Klein,²¹ A. G. Knospe,⁵² A. Kocoloski,²² D. D. Koetke,⁴⁶ T. Kollegger,¹² J. Konzer,³³ M. Kopytine,¹⁸ I. Koralt,²⁹ W. Korsch,¹⁹ L. Kotchenda,²⁵ V. Kouchpil,¹¹ P. Kravtsov,²⁵ K. Krueger,¹ M. Krus,¹⁰ L. Kumar,³⁰ P. Kurnadi,⁶ M. A. C. Lamont,³ J. M. Landgraf,³ S. LaPointe,⁵⁰ J. Lauret,³ A. Lebedev,³ R. Lednicky,¹⁷ C.-H. Lee,³⁴ J. H. Lee,³ W. Leight,²² M. J. LeVine,³ C. Li,³⁸ L. Li,⁴³ N. Li,⁵¹ W. Li,⁴⁰ X. Li,³³ X. Li,³⁹ Y. Li,⁴⁴ Z. Li,⁵¹ G. Lin,⁵² S. J. Lindenbaum,²⁶ M. A. Lisa,²⁸ F. Liu,⁵¹ H. Liu,⁵ J. Liu,³⁶ T. Ljubicic,³ W. J. Llope,³⁶ R. S. Longacre,³ W. A. Love,³ Y. Lu,³⁸ G. L. Ma,⁴⁰ Y. G. Ma,⁴⁰ D. P. Mahapatra,¹³ R. Majka,⁵² O. I. Mall,⁵ L. K. Mangotra,¹⁶ R. Manweiler,⁴⁶ S. Margetis,¹⁸ C. Markert,⁴³ H. Masui,²¹ H. S. Matis,²¹ Yu. A. Matulenko,³² D. McDonald,³⁶ T. S. McShane,⁹ A. Meschanin,³² R. Milner,²² N. G. Minaev,³² S. Mioduszewski,⁴² A. Mischke,²⁷ M. K. Mitrovski,¹² B. Mohanty,⁴⁷ M. M. Mondal,⁴⁷ D. A. Morozov,³² M. G. Munhoz,³⁷ B. K. Nandi,¹⁴ C. Nattrass,⁵² T. K. Nayak,⁴⁷ J. M. Nelson,² P. K. Netrakanti,³³ M. J. Ng,⁴ L. V. Nogach,³² S. B. Nurushhev,³² G. Odyniec,²¹ A. Ogawa,³ H. Okada,³ V. Okorokov,²⁵ D. Olson,²¹ M. Pachr,¹⁰ B. S. Page,¹⁵ S. K. Pal,⁴⁷ Y. Pandit,¹⁸ Y. Panebratsev,¹⁷ T. Pawlak,⁴⁸ T. Peitzmann,²⁷ V. Perevoztchikov,³ C. Perkins,⁴ W. Peryt,⁴⁸ S. C. Phatak,¹³ P. Pile,³ M. Planinic,⁵³ M. A. Ploskon,²¹ J. Pluta,⁴⁸ D. Plyku,²⁹ N. Poljak,⁵³ A. M. Poskanzer,²¹ B. V. K. S. Potukuchi,¹⁶ C. B. Powell,²¹ D. Prindle,⁴⁹ C. Pruneau,⁵⁰ N. K. Pruthi,³⁰ P. R. Pujahari,¹⁴ J. Putschke,⁵² R. Raniwala,³⁵ S. Raniwala,³⁵ R. L. Ray,⁴³ R. Redwine,²² R. Reed,⁵ J. M. Rehberg,¹² H. G. Ritter,²¹ J. B. Roberts,³⁶ O. V. Rogachevskiy,¹⁷ J. L. Romero,⁵ A. Rose,²¹ C. Roy,⁴¹ L. Ruan,³ M. J. Russcher,²⁷ R. Sahoo,⁴¹ S. Sakai,⁶ I. Sakrejda,²¹ T. Sakuma,²² S. Salur,⁵ J. Sandweiss,⁵² E. Sangaline,⁵ J. Schambach,⁴³ R. P. Scharenberg,³³ N. Schmitz,²³ T. R. Schuster,¹² J. Seele,²² J. Seger,⁹ I. Selyuzhenkov,¹⁵ P. Seyboth,²³ E. Shahaliev,¹⁷ M. Shao,³⁸ M. Sharma,⁵⁰ S. S. Shi,⁵¹ E. P. Sichtermann,²¹ F. Simon,²³ R. N. Singaraju,⁴⁷ M. J. Skoby,³³ N. Smirnov,⁵² P. Sorensen,³ J. Sowinski,¹⁵ H. M. Spinka,¹ B. Srivastava,³³ T. D. S. Stanislaus,⁴⁶ D. Staszak,⁶ J. R. Stevens,¹⁵ R. Stock,¹² M. Strikhanov,²⁵ B. Stringfellow,³³ A. A. P. Suaide,³⁷ M. C. Suarez,⁸ N. L. Subba,¹¹ M. Sumner,²¹ X. M. Sun,²¹ Y. Sun,³⁸ Z. Sun,²⁰ B. Surrow,²² T. J. M. Symons,²¹ A. Szanto de Toledo,³⁷ J. Takahashi,⁷ A. H. Tang,³ Z. Tang,³⁸ L. H. Tarini,⁵⁰ T. Tarnowsky,²⁴ D. Thein,⁴³ J. H. Thomas,²¹ J. Tian,⁴⁰ A. R. Timmins,⁵⁰ S. Timoshenko,²⁵ D. Tlusty,¹¹ M. Tokarev,¹⁷ T. A. Trainor,⁴⁹ V. N. Tram,²¹ S. Trentalange,⁶ R. E. Tribble,⁴² O. D. Tsai,⁶ J. Ulery,³³ T. Ullrich,³ D. G. Underwood,¹ G. Van Buren,³ G. van Nieuwenhuizen,²² J. A. Vanfossen, Jr.,¹⁸ R. Varma,¹⁴ G. M. S. Vasconcelos,⁷ A. N. Vasiliev,³² F. Videbaek,³ Y. P. Viyogi,⁴⁷ S. Vokal,¹⁷ S. A. Voloshin,⁵⁰ M. Wada,⁴³ M. Walker,²² F. Wang,³³ G. Wang,⁶ H. Wang,²⁴ J. S. Wang,²⁰ Q. Wang,³³ X. L. Wang,³⁸ Y. Wang,⁴⁴ G. Webb,¹⁹ J. C. Webb,³

G. D. Westfall,²⁴ C. Whitten Jr.,⁶ H. Wieman,²¹ E. Wingfield,⁴³ S. W. Wissink,¹⁵ R. Witt,⁴⁵ Y. Wu,⁵¹ W. Xie,³³ N. Xu,²¹ Q. H. Xu,³⁹ W. Xu,⁶ Y. Xu,³⁸ Z. Xu,³ L. Xue,⁴⁰ Y. Yang,²⁰ P. Yepes,³⁶ K. Yip,³ I-K. Yoo,³⁴ Q. Yue,⁴⁴ M. Zawisza,⁴⁸ H. Zbroszczyk,⁴⁸ W. Zhan,²⁰ S. Zhang,⁴⁰ W. M. Zhang,¹⁸ X. P. Zhang,²¹ Y. Zhang,²¹ Z. P. Zhang,³⁸ J. Zhao,⁴⁰ C. Zhong,⁴⁰ J. Zhou,³⁶ W. Zhou,³⁹ X. Zhu,⁴⁴ Y. H. Zhu,⁴⁰ R. Zoulkarneev,¹⁷ and Y. Zoulkarneeva¹⁷

(STAR Collaboration)

- ¹Argonne National Laboratory, Argonne, Illinois 60439, USA
²University of Birmingham, Birmingham, United Kingdom
³Brookhaven National Laboratory, Upton, New York 11973, USA
⁴University of California, Berkeley, California 94720, USA
⁵University of California, Davis, California 95616, USA
⁶University of California, Los Angeles, California 90095, USA
⁷Universidade Estadual de Campinas, Sao Paulo, Brazil
⁸University of Illinois at Chicago, Chicago, Illinois 60607, USA
⁹Creighton University, Omaha, Nebraska 68178, USA
¹⁰Czech Technical University in Prague, FNSPE, Prague, 115 19, Czech Republic
¹¹Nuclear Physics Institute AS CR, 250 68 Řež/Prague, Czech Republic
¹²University of Frankfurt, Frankfurt, Germany
¹³Institute of Physics, Bhubaneswar 751005, India
¹⁴Indian Institute of Technology, Mumbai, India
¹⁵Indiana University, Bloomington, Indiana 47408, USA
¹⁶University of Jammu, Jammu 180001, India
¹⁷Joint Institute for Nuclear Research, Dubna, 141 980, Russia
¹⁸Kent State University, Kent, Ohio 44242, USA
¹⁹University of Kentucky, Lexington, Kentucky, 40506-0055, USA
²⁰Institute of Modern Physics, Lanzhou, China
²¹Lawrence Berkeley National Laboratory, Berkeley, California 94720, USA
²²Massachusetts Institute of Technology, Cambridge, MA 02139-4307, USA
²³Max-Planck-Institut für Physik, Munich, Germany
²⁴Michigan State University, East Lansing, Michigan 48824, USA
²⁵Moscow Engineering Physics Institute, Moscow Russia
²⁶City College of New York, New York City, New York 10031, USA
²⁷NIKHEF and Utrecht University, Amsterdam, The Netherlands
²⁸Ohio State University, Columbus, Ohio 43210, USA
²⁹Old Dominion University, Norfolk, VA, 23529, USA
³⁰Panjab University, Chandigarh 160014, India
³¹Pennsylvania State University, University Park, Pennsylvania 16802, USA
³²Institute of High Energy Physics, Protvino, Russia
³³Purdue University, West Lafayette, Indiana 47907, USA
³⁴Pusan National University, Pusan, Republic of Korea
³⁵University of Rajasthan, Jaipur 302004, India
³⁶Rice University, Houston, Texas 77251, USA
³⁷Universidade de Sao Paulo, Sao Paulo, Brazil
³⁸University of Science & Technology of China, Hefei 230026, China
³⁹Shandong University, Jinan, Shandong 250100, China
⁴⁰Shanghai Institute of Applied Physics, Shanghai 201800, China
⁴¹SUBATECH, Nantes, France
⁴²Texas A&M University, College Station, Texas 77843, USA
⁴³University of Texas, Austin, Texas 78712, USA
⁴⁴Tsinghua University, Beijing 100084, China
⁴⁵United States Naval Academy, Annapolis, MD 21402, USA
⁴⁶Valparaiso University, Valparaiso, Indiana 46383, USA
⁴⁷Variable Energy Cyclotron Centre, Kolkata 700064, India
⁴⁸Warsaw University of Technology, Warsaw, Poland
⁴⁹University of Washington, Seattle, Washington 98195, USA
⁵⁰Wayne State University, Detroit, Michigan 48201, USA
⁵¹Institute of Particle Physics, CCNU (HZNU), Wuhan 430079, China
⁵²Yale University, New Haven, Connecticut 06520, USA
⁵³University of Zagreb, Zagreb, HR-10002, Croatia

(Dated: December 9, 2009)

Charged-particle spectra associated with direct photon (γ_{dir}) and π^0 are measured in $p+p$ and Au+Au collisions at center-of-mass energy $\sqrt{s_{NN}} = 200$ GeV with the STAR detector at RHIC. A

shower-shape analysis is used to partially discriminate between γ_{dir} and π^0 . Assuming no associated charged particles in the γ_{dir} direction (near side) and small contribution from fragmentation photons (γ_{frag}), the associated charged-particle yields opposite to γ_{dir} (away side) are extracted. At mid-rapidity ($|\eta| < 0.9$) in central Au+Au collisions, charged-particle yields associated with γ_{dir} and π^0 at high transverse momentum ($8 < p_T^{trig} < 16$ GeV/c) are suppressed by a factor of 3-5 compared with $p+p$ collisions. The observed suppression of the associated charged particles, in the kinematic range $|\eta| < 1$ and $3 < p_T^{assoc} < 16$ GeV/c, is similar for γ_{dir} and π^0 , and independent of the γ_{dir} energy within uncertainties. These measurements indicate that the parton energy loss, in the covered kinematic range, is insensitive to the parton path length.

PACS numbers: 25.75.-q, 25.75.Bh

Keywords: hard scattering, relativistic heavy-ion collisions, jets, direct photons, energy loss mechanism

A major goal of measurements at the Relativistic Heavy Ion Collider (RHIC) is to quantify the properties of the QCD matter created in heavy-ion collisions at high energy [1]. One key property is the medium energy density, which can be probed by its effect on a fast parton propagating through it [2]. A parton scattered in the initial stages of a heavy-ion collision propagates through the medium and results in a shower of hadrons (jet), with high transverse momenta (p_T), in the detectors. The medium energy density is extracted through the comparison of measured observables with theoretical models. Many perturbative Quantum Chromodynamics (pQCD)-based models of parton energy loss have successfully described much of the high- p_T data with medium parameters that span a wide range [3]. To better constrain these parameters, it is essential to examine the dependence of the energy loss (ΔE) on the initial energy of the parton (E), path length of the parton through the medium (L), and the parton type, independently. This necessitates additional experimental observables.

The γ_{dir} -jet coincidence measurements have long been proposed as a powerful tool to study parton energy loss in the medium created at RHIC [4]. The leading-order production processes of direct photons γ_{dir} , quark-gluon Compton scattering ($q + g \rightarrow q + \gamma$) and quark-antiquark annihilation ($q + \bar{q} \rightarrow g + \gamma$), are free from the uncertainties accompanying fragmentation. The outgoing high- p_T γ balances the p_T of the partner parton separated by π in azimuth (“away-side”), modulo negligible corrections due to parton intrinsic p_T [5]. The study of the spectra of the away-side jet particles associated with the high- p_T γ_{dir} can constrain the dependence of ΔE on E . The mean-free path of the γ in the medium is large enough that its momentum is preserved, regardless of the position of the initial scattering vertex. The γ does not suffer from the geometric biases (non-uniform spatial sampling of hadron triggers due to energy loss in the medium) inherent in single hadron spectra and di-hadron azimuthal correlation measurements. A comparison between the spectra of the away-side particles associated with γ_{dir} vs. those associated with π^0 can constrain the dependence of ΔE on L [6].

In this Letter we examine ΔE by comparing jet yields measured in central Au+Au collisions and $p+p$ collisions

at $\sqrt{s_{NN}} = 200$ GeV via correlations in azimuthal angle between particles. We investigate the ΔE dependence on E , via γ_{dir} -charged-particle (γ_{dir} - h^\pm) correlations, and on L , via a comparison of π^0 -charged particle (π^0 - h^\pm) to (γ_{dir} - h^\pm) correlations. Taking advantage of the unique configuration of the STAR detector, we present a novel analysis technique to extract the spectra of charged particles associated with γ_{dir} . This technique provides a much needed higher statistics than that in [7] for these types of rare probes, and allows for more statistically significant measurement.

The STAR detector is well suited for measuring azimuthal angular correlations due to the large coverage in pseudorapidity (η) and full coverage in azimuth (ϕ). Using the Barrel Electromagnetic Calorimeter (BEMC) [8] to select events (*i.e.* “trigger”) with high- p_T γ , the STAR experiment collected an integrated luminosity of $535 \mu\text{b}^{-1}$ of Au+Au collisions in 2007 and 11 pb^{-1} of $p+p$ collisions in 2006. The BEMC consists of 4800 channels (towers) and measures the γ energy. The Time Projection Chamber (TPC) [9] detects charged-particle tracks. A crucial part of the analysis is to discriminate between showers from γ_{dir} and two close γ 's from high- p_T π^0 symmetric decays. At $p_T^{\pi^0} \sim 8$ GeV/c, the angular separation between the two γ 's resulting from a π^0 decay is typically smaller than a tower size, but a π^0 shower is generally broader than a single γ shower. The Barrel Shower Maximum Detector (BSMD) [8] consists of 18000 channels (strips) in each plane (η and ϕ) and resides at ~ 5.6 radiation lengths inside the calorimeter towers. The BSMD is capable of $(2\gamma)/(1\gamma)$ separation up to $p_T^{\pi^0} \sim 26$ GeV/c due to its high granularity.

In this analysis, events with vertex within ± 55 cm of the center of TPC are selected. The BEMC is calibrated using the 2006 $p+p$ data, using a procedure described elsewhere [10]. The tracking efficiency of charged particles as a function of event multiplicity is determined by embedding π^\pm in real data. The effects of energy and momentum resolution are estimated to be small compared to other systematic uncertainties in this analysis, and no correction is applied. The charged-track quality criteria are similar to those used in previous STAR analyses [11]. Events with at least one electromagnetic cluster (defined as 1 or 2 towers) with $E_T > 8$ GeV are

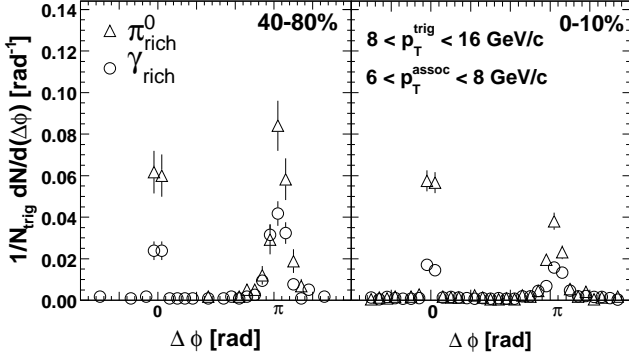


FIG. 1: Correlations (without background subtraction) of γ_{rich} sample of triggers and π_{rich}^0 sample with associated charged hadrons in peripheral (40-80%) and central (0-10%) Au+Au collisions.

selected. A trigger tower is rejected if it has a track with $p > 3.0$ GeV/c pointing to it. The π^0/γ discrimination depends on an analysis of the shower shape as measured by the BSMD and BEMC. The shower shape is studied by single-particle Monte-Carlo simulation and embedding γ and π^0 in real data. The shower shape is quantified with the cluster energy, measured by the BEMC, normalized by the position-dependent energy moment, measured by the BSMD strips. The shower profile cuts were tuned to obtain a γ_{dir} -free (π_{rich}^0) sample and a sample rich in γ_{dir} (γ_{rich}). From embedding single γ 's and π^0 's into Au+Au data, the rejection power of the shower profile cuts is estimated to be $> 99\%$ for rejecting γ_{dir} and $\sim 60\%$ for rejecting π^0 . A detailed study of the shower profile, primary vertex, and charge-rejection cuts is performed to determine the systematic uncertainties, which also include the energy scale uncertainty.

The correlations in $\Delta\phi$ between particles, measured as the number of associated particles per trigger per $\Delta\phi$ ("correlation functions"), are used in both $p+p$ and Au+Au collisions to determine the (jet) associated particle yields. Figure 1 shows the correlation functions for γ_{rich} and π_{rich}^0 triggers for the peripheral (largest impact parameters) and most central (smallest impact parameters) bins in Au+Au collisions. As expected the γ_{rich} -triggered sample has lower near-side yields than those of the π_{rich}^0 , but not zero. In addition to the isotropically distributed underlying-event background, the non-zero near-side yield for the γ_{rich} sample is expected due to remaining background contributions of widely separated γ 's that are correlated with charged particles. The shower-shape analysis is only effective for rejecting two close γ showers, leaving background γ 's from asymmetric decays of π^0 and η , and fragmentation γ 's.

The uncorrelated background level is subtracted, assuming an isotropic distribution determined by fitting the correlation function with two Gaussians and a con-

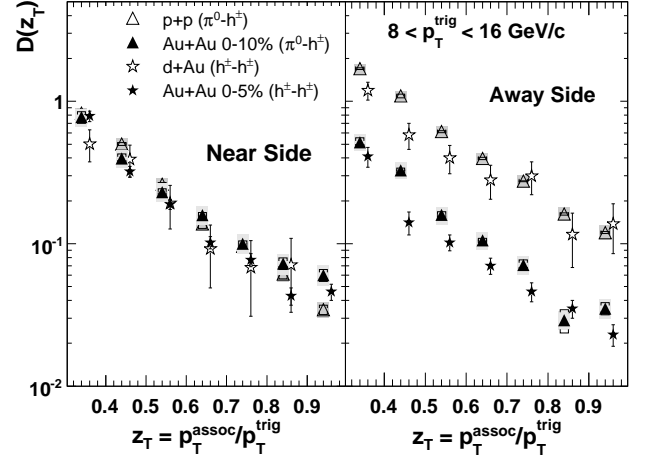


FIG. 2: The z_T dependence of $\pi^0 - h^\pm$ and $h^\pm - h^\pm$ [11] near-side (left panel) and away-side (right panel) associated particle yields. The bin centers are shifted for clarity. The shaded boxes show the systematic errors correlated in z_T , and the brackets show the point-to-point systematic errors.

stant. Over the measured range of p_T^{assoc} the expected modulation in the background shape, due to the correlation with respect to the reaction plane in heavy-ion collisions, is found to have a negligible effect on the subtraction. As shown in Fig. 1, the level of uncorrelated background is dramatically suppressed relative to the signal. The near- and away-side yields, Y^n and Y^a , of associated particles per trigger are extracted by integrating the $1/N_{trig} dN/d(\Delta\phi)$ distributions, over $|\Delta\eta| < 1.9$, in $|\Delta\phi| \leq 0.63$ and $|\Delta\phi - \pi| \leq 0.63$, respectively. The yield is corrected for the tracking efficiency of charged particles as a function of event multiplicity but, as in [11], not for acceptance due to the η cuts.

Figure 2 shows the hadron yields associated with π_{rich}^0 normalized by the measured number of triggers ($D(z_T)$ [4]), as a function of $z_T = p_T^{assoc}/p_T^{trig}$, compared to the yields per charged-hadron trigger [11]. The yield in the first z_T bin is corrected for the Δz_T width sampled on a trigger-by-trigger basis. The systematic errors on the π_{rich}^0 -triggered yields have a correlated component of $\sim 7 - 13\%$, and point-to-point uncertainties that are less than 5% for much of the data. Since the charged-hadron triggers are dominated by charged pions, the associated yields are expected to be similar to those of π^0 triggers, although there could be some differences due to the presence of proton triggers in the charged-trigger sample. A general agreement of $\sim 20 - 30\%$ between the results from this analysis ($\pi^0 - h^\pm$) and the previous STAR analysis ($h^\pm - h^\pm$) is clearly seen in both panels of Fig. 2, indicating the π_{rich}^0 -sample is free of γ_{dir} .

Assuming zero near-side yield for γ_{dir} triggers and a sample of π^0 free of γ_{dir} , the away-side yield of hadrons

correlated with the γ_{dir} is extracted as

$$Y_{\gamma_{dir}+h} = \frac{Y_{\gamma_{rich}+h}^a - \mathcal{R}Y_{\gamma_{rich}+h}^n}{1-r}, \text{ where } \mathcal{R} = \frac{Y_{\pi_{rich}+h}^a}{Y_{\pi_{rich}+h}^n},$$

$$r = \frac{Y_{\gamma_{rich}+h}^n}{Y_{\pi_{rich}+h}^n}, \text{ and } 1-r = \frac{N^{\gamma_{dir}}}{N^{\gamma_{rich}}}. \quad (1)$$

Here, $Y_{\gamma_{rich}+h}^a$ and $Y_{\pi_{rich}+h}^a$ are the away (near)-side yields of associated particles per γ_{rich} and π_{rich}^0 triggers, respectively. The ratio r is equivalent to the fraction of “background” triggers in the γ_{rich} trigger sample, and $N^{\gamma_{dir}}$ and $N^{\gamma_{rich}}$ are the numbers of γ_{dir} and γ_{rich} triggers, respectively. The value of r is found to be $\sim 55\%$ in $p+p$ and decreases to $\sim 30\%$ in central Au+Au with little dependence on p_T^{trig} . All background to γ_{dir} is subtracted with the assumption that the background triggers have the same correlation function as the π_{rich}^0 sample. PYTHIA simulations [12] indicate that correlations of γ triggers from asymmetric hadron decays are similar, to within $\sim 10\%$, to those of symmetrically decaying π^0 triggers as well as the measured correlations of π_{rich}^0 triggers, at the same p_T^{trig} . On the other hand, PYTHIA shows that the γ_{frag} has a different correlation with the charged particle compared to that of π^0 with insensitivity to the charged rejection cut. However, the γ_{frag} contribution is expected to fall off more rapidly in x_T ($x_T = 2p_T/\sqrt{s}$) than the other lowest order γ_{dir} 's [13]. One theoretical calculation [14] shows the ratio of γ_{frag} to γ_{dir} to be $\sim 30 - 40\%$ at $p_T^{\gamma} > 8$ GeV/c in $p+p$ at mid-rapidity at RHIC energy.

For the γ_{dir} -triggered yields, the systematic errors are evaluated similar to π^0 and summarized as a function of centrality and z_T in Table I. An additional source of un-

TABLE I: Systematic errors on γ_{dir} -triggered yields.

| Au+Au 0-10% collisions z_T -correlated error: 17-19% | | | | | | | |
|--|------|------|------|------|------|------|--|
| z_T bin | 0.35 | 0.45 | 0.55 | 0.65 | 0.75 | 0.85 | |
| point-to-point error (%) | 37 | 21 | 21 | 55 | 20 | 49 | |
| pp collisions z_T -correlated error: 11-13% | | | | | | | |
| z_T bin | 0.35 | 0.45 | 0.55 | 0.65 | 0.75 | 0.85 | |
| point-to-point error (%) | 10 | 13 | 16 | 93 | 17 | 24 | |

certainty on these yields arises from the assumption that the background contribution of γ_{frag} in the γ_{rich} triggers has the same correlation as the π_{rich}^0 triggers. This is assessed by comparing (with a χ^2 analysis) the shape of the near-side correlation of γ_{rich} to π_{rich}^0 triggers. Thus, excepting those γ_{frag} that have no near-side yield, the contribution of γ_{frag} in the γ_{rich} sample, not satisfying the assumption, is taken into account in the systematic errors.

Figure 3 (upper panel) shows the z_T dependence of the trigger-normalized fragmentation function for $(\pi^0 - h^{\pm})_{215}$ and $(\gamma - h^{\pm})$ in $p+p$, and 0-10% central Au+Au colli-

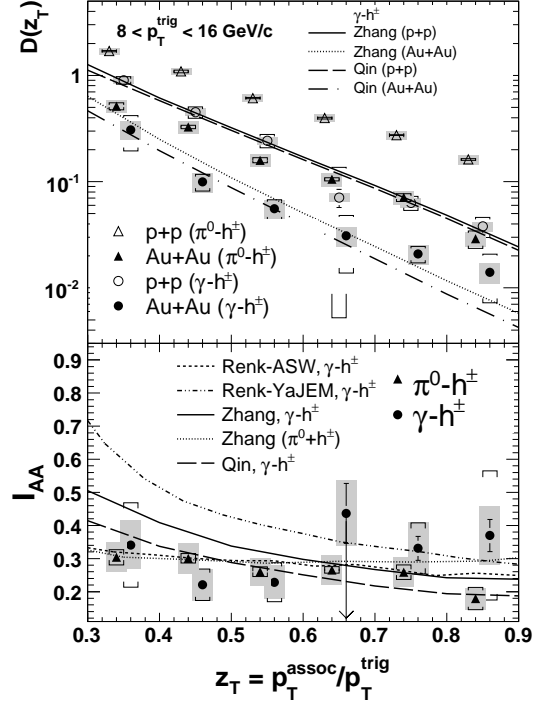


FIG. 3: Upper panel: z_T dependence of away-side associated-particle yields for π^0 triggers (triangles) and γ_{dir} triggers (circles) for $p+p$ (open symbols) and 0-10% Au+Au (closed symbols) collisions. The trigger particle has $8 < E_T^{trig} < 16$ GeV/c. Lower panel: z_T dependence of I_{AA} for γ_{dir} triggers (circles) and π^0 triggers (triangles). Boxes show the z_T -correlated systematic errors, and brackets show the point-to-point systematic errors. The bin centers are shifted for clarity. Data is compared to theoretical calculations (see text).

sions. At a given z_T , the away-side yield per π^0 trigger is significantly larger than the yield per γ_{dir} trigger. This difference is expected, since the γ_{dir} carries the total scattered constituent momentum while the π^0 carries only a fraction of it. In addition, there are different proportions of quarks and gluons recoiling from γ_{dir} and π^0 triggers. In Au+Au collisions, partonic energy loss can lead to additional differences on the away-side since the path length, the energy of the parton, and the partonic species composition of the recoiling parton are different between γ_{dir} and π^0 triggers at the same p_T^{trig} . A comparison to two different theoretical calculations of the associated yields for γ_{dir} triggers is shown in Fig. 3 (upper panel). The calculation by Zhang [15] does not include γ_{frag} and describes the data well. The calculation by Qin [16] includes a significant contribution of γ_{frag} , but it is quite similar in yield for $p+p$ and also describes the data within current uncertainties.

In order to quantify the away-side suppression, we calculate the quantity I_{AA} , which is defined as the ratio of the integrated yield of the away-side associated particles per trigger particle in Au+Au to that in $p+p$ collisions. Figures 3 (lower panel) and 4 show I_{AA} as a function

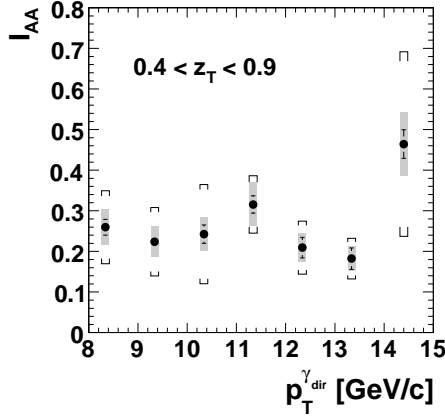


FIG. 4: I_{AA} as a function of p_T for γ_{dir} triggers, measured in 0-10% Au+Au collisions. The associated charged particles have $z_T = 0.4 - 0.9$. The shaded boxes show the systematic errors correlated in p_T^{trig} , and the brackets show the point-to-point systematic errors.

of z_T and p_T^{trig} , respectively. Despite the differences between $\pi^0 - h^\pm$ and $\gamma - h^\pm$, seen in Fig. 3 (upper panel), the value of $I_{AA}^{\gamma-h^\pm}$ is z_T independent and similar to that of $I_{AA}^{\pi^0-h^\pm}$. The $I_{AA}^{\gamma-h^\pm}$ agrees well with theoretical calculations in which the energy loss is tuned to the single- and di-hadron measurements [11, 17]. The calculation by Zhang for both γ_{dir} and π^0 triggers [15] shows only a small difference in the suppression factor, growing at low z_T . Two calculations for γ_{dir} triggers, labeled as Qin [16] and Renk-ASW [18], show even less of a rise at low z_T . In the calculation [18] using the ASW implementation of energy loss [19], the effect of fluctuations in energy loss dominates over the effect of geometry, explaining the similarity in γ - and π^0 -associated yields. The calculation that is not consistent with the data at low z_T , the Renk-YaJEM model [18], differs in that the lost energy is tracked and redistributed through the medium. The disagreement with this model may indicate that the lost energy is distributed to extremely low p_T and large angles [18] (as also evidenced by hadron-hadron correlation measurements [20]), and perhaps even that the correlations to the trigger particle are lost. To further test this, one must explore the region of low z_T .

Figure 4 addresses the E dependence of ΔE . The suppression of the away-side multiplicity per γ_{dir} trigger in Au+Au relative to $p+p$ collisions shows no strong p_T^{trig} dependence, which indicates no strong E dependence in the measured p_T range.

In summary, $\gamma_{dir} - h$ correlation measurements are reported by the STAR collaboration, providing important new constraints on theoretical models. The agreement between the measured $I_{AA}^{\gamma-h^\pm}$ and $I_{AA}^{\pi^0-h^\pm}$ in the covered kinematic range could theoretically be due to an interplay of compensating factors of the dependence of energy

loss on the initial parton energy, the energy loss of gluons vs. quarks, and the energy loss path-length dependence. The measurement of the dependence of $I_{AA}^{\gamma-h^\pm}$ on p_T^{trig} , however, shows no significant dependence on the initial parton energy. Therefore, the dependence of observable parton energy loss on parton species and path length traversed by the parton in the medium must be similarly small.

We thank the RHIC Operations Group and RCF at BNL, the NERSC Center at LBNL and the Open Science Grid consortium for providing resources and support. This work was supported in part by the Offices of NP and HEP within the U.S. DOE Office of Science, the U.S. NSF, the Sloan Foundation, the DFG cluster of excellence ‘Origin and Structure of the Universe’, CNRS/IN2P3, STFC and EPSRC of the United Kingdom, FAPESP CNPq of Brazil, Ministry of Ed. and Sci. of the Russian Federation, NNSFC, CAS, MoST, and MoE of China, GA and MSMT of the Czech Republic, FOM and NWO of the Netherlands, DAE, DST, and CSIR of India, Polish Ministry of Sci. and Higher Ed., Korea Research Foundation, Ministry of Sci., Ed. and Sports of the Rep. Of Croatia, Russian Ministry of Sci. and Tech, and RosAtom of Russia.

-
- [1] J. Adams et al., Nucl. Phys. A **757**, 102 (2005).
 - [2] M. Gyulassy, P. Levai and I. Vitev, Phys. Lett. B **538**, 282 (2002).
 - [3] S. A. Bass et al., Phys. Rev. C **79**, 024901 (2009).
 - [4] X.-N. Wang, Z. Huang and I. Sarcevic, Phys. Rev. Lett. **77**, 231 (1996).
 - [5] L. Cornell and J. F. Owens, Phys. Rev. D **22**, 1609 (1980) and references therein.
 - [6] T. Renk and K. Eskola, Phys. Rev. C **75**, 054910 (2007).
 - [7] A. Adare et al., Phys. Rev. C **80**, 024908 (2009).
 - [8] M. Beddo et al., Nucl. Instrum. Meth. A **499**, 725 (2003).
 - [9] M. Anderson et al., Nucl. Instrum. Meth. A **499**, 659 (2003).
 - [10] B. I. Abelev et al., long article on π^0 , γ , and η production, arxiv no. TBD.
 - [11] J. Adams et al., Phys. Rev. Lett. **97**, 162301 (2006).
 - [12] T. Sjöstrand, S. Mrenna and P. Skands, Comput. Phys. Commun. **178**, 852 (2008) [PYTHIA v8.1].
 - [13] G. Sterman et al., Rev. Mod. Phys. **67**, 157 (1995).
 - [14] D. de Florian and W. Vogelsang, Phys. Rev. D **72**, 014014 (2005).
 - [15] H. Zhang et al., Nucl. Phys. A **830**, 443c (2009).
 - [16] G.-Y. Qin et al., Phys. Rev. C **80**, 054909 (2009).
 - [17] S.S. Adler et al., Phys. Rev. Lett. **91**, 072301 (2003).
 - [18] T. Renk, Phys. Rev. C **80**, 014901 (2009).
 - [19] C.A. Salgado and U.A. Wiedemann, Phys. Rev. D **68**, 014008 (2003).
 - [20] J. Adams et al., Phys. Rev. Lett. **95**, 152301 (2005); A. Adare et al., Phys. Rev. C **78**, 014901 (2008).